Int. J. Heat Mass Transfer. Vol. 8, pp. 1515–1535. Pergamon Press 1965. Printed in Great Britain

LAMINAR FLOW BETWEEN PARALLEL FLAT PLATES, WITH HEAT TRANSFER, OF WATER WITH VARIABLE PHYSICAL PROPERTIES

G. POOTS*
Department of Theoretical Mechanics, University of Bristol
and
M. H. ROGERS
Computer Unit, University of Bristol

(*Received* 19 *December* 1964 *and in revised form* 22 *April* 1965)

Abstract—The laminar fully developed flow of water in a vertical channel is examined, using the complete equations of motion with experimental values (in the range 0–100°C) for the viscosity, conductivity, specific heat, and density. Although the local effects of variations in these quantities are, of course, small, the cumulative effect is significant for moderate temperature differences. Accordingly, emphasis has been placed on the evaluation of integrated properties such as mass flow and heat transfer.

Poiseuille, Couette and mixed Poiseuille–Couette flows are investigated for a range of wall temperature differences and the effects of the temperature dependent properties on the velocity and thermal profiles are discussed in detail. Wall Nusselt numbers, flow rates, skin friction coefficients, friction factors and Reynolds analogy factors are evaluated for all these regimes.

NOMENCLATURE

A_i, B_i, C_i, D_i, coefficients;
C_p, specific heat at constant pressure, cal/g degC;
d, distance between the plates, cm;
$E_r = N_r^2/Jc_p(T_1 - T_0)$, Eckert number;
g, acceleration due to gravity;
$G_r = -\rho_r(\rho_1 - \rho_0)gd^3/\mu_r^2$, Grashof number;
k, thermal conductivity, cal/s cm degC;
$n = V/N_r$, dimensionless velocity of the plate;
$N_r = \frac{d^2}{2\mu_r}\left[-\frac{dp_D}{dx}\right]$, representative velocity related to the pressure gradient, cm/s;
Nu, Nusselt number;
p, pressure;
$Pr = \mu C_p/k$, Prandtl number;
$Re_r = \rho_r N_r d/\mu_r$, Reynolds number;
$Nu/C_f Re_r$, Reynolds factor;
T, temperature, °C;
u, velocity, cm/s;
$U = u/N_r$, dimensionless velocity;
$V = nN_r$, velocity of plate at $y = d$;
W, flow rate, g/s;
x, y, z, Cartesian co-ordinates, cm;
$Y = y/d$, dimensionless co-ordinate.

Greek symbols

α, β, constants of integration;
β_r, coefficient of volumetric expansion, 1/degC;
$\gamma_r = E_r Pr_r$, a dimensionless quantity;
μ, viscosity, g/cm s;
ρ, density, g/cm³;
$\Theta = (T - T_0)/(T_1 - T_0)$, dimensionless temperature.

Subscripts

1, 2, wall condition at $y = 0$, d respectively;
r, reference condition;
D, dynamic condition.

* Present address: Department of Applied Mathematics, University of Hull.

1. INTRODUCTION

THE MOST commonly used coolants in heat-transfer appliances are probably air and water.

A great deal of theoretical information on basic laminar flow and heat-transfer problems involving air now exists in the literature. In particular for the compressible laminar boundary layer (see Stewartson [1]) calculations have been performed with due allowance for variable physical properties. Moreover, the study of a model gas having similar overall variable physical properties has proved extremely fruitful, since the equations of motion are then more tractable analytically and are more amenable to numerical analysis.

To date it does not appear from the literature that the present quantitative knowledge of laminar flow with heat transfer in liquids is as satisfactory. One of the essential difficulties is that the properties of the two main classifications, namely metallic and non-metallic liquids are widely different. Even for the class of non-metallic liquids the results obtained for a given flow and heat-transfer configuration with a high viscosity liquid are expected to differ from those obtained using a low viscosity liquid; for example, in the former viscous dissipation may cause appreciable changes, whilst in the latter it is negligible.

However, considerable progress has been made in obtaining quantitative information on the effects of temperature-dependent viscosity in liquids. Attention has been given to the flow of oil between a journal and its bearing. As oil has a high viscosity significant changes in velocity and thermal profiles occur due to a temperature rise produced by viscous dissipation. Such effects have been considered in detail by Vogelpohl [2], Nahme [3], Hausenblas [4] and by Targ [5]. In these references the conductivity and density of the oil were assumed independent of the temperature and the viscosity–temperature dependence was taken either in the form

$$\mu^{-1} = a + bT \quad \text{or} \quad \mu = a \exp(bT),$$

where a and b are constants determined from experimental data.

Another class of problem which has received quite considerable treatment in the literature is the forced convection by laminar flow in ducts and tubes. The work of Deissler [6] deals with the fully developed velocity and thermal profiles for the flow of liquid metals in a circular tube; here it is assumed that the heat-transfer rate varies slowly along the tube in the flow direction and the fluid properties are variable along the radius. Maslen [7] has discussed the fully developed combined free and forced convection between vertical flat plates, which are maintained at constant temperature. In this work the variation of conductivity with temperature is neglected and the μ and ρ dependence was approximated by the relations:

$$\mu^{-1} = a + bT, \quad \rho = \rho_r[1 - \beta_r(T - T_r)].$$

It should be noted that the latter approximation to the equation of state enables the flow and heat transfer to be evaluated without *a priori* information on T_r, the reference inlet temperature. Subject to the above relations Maslen presents an exact solution of the equations of motion when viscous dissipation is neglected.

Allowing for a linear variation of viscosity with temperature the classical constant property Graetz solution for the thermal entrance length has been re-investigated. For a step change in wall temperature, an iterative procedure based on the isothermal solution as a first approximation has been used by Boelter *et al.* [8], Yamagata [9], and Pigford [10] to obtain first-order corrections in the velocity profile. Yamagata [9] and Pigford [10] have also obtained first-order corrections in local heat-transfer coefficients at the start of the inlet region, where the velocity profile may be approximated by a linear function. The thermal entrance region for a circular tube has been further treated by Yang [11] using the Pohlhausen type integral techniques of boundary layer theory. Yang treats the cases of a step change in wall temperature and a step change in wall heat flux. In his analysis the viscosity–temperature dependence is taken to be $\mu^{-1} = a + bT$; the inertia terms and density variations are neglected in the momentum equation; and finally viscous dissipation and heat transfer by radial convection are neglected in the energy equation, where the conductivity is taken to be constant. It should be noted that in the work of Pigford [10] buoyancy effects are included on assuming that the density varies linearly with temperature.

The above heat-transfer problems have been investigated using relatively simple relationships for the variation of viscosity with temperature.

Most liquids have a definite non-linear viscosity variation with temperature and this is true, but to a much less degree, of the temperature variations in density, conductivity and specific heat. It is clear that a more careful study should be made of the validity of many of the approximations used in the solution of these problems. However, a variable fluid property problem in free convection has been successfully solved by Sparrow and Gregg [12]. Here the free convection flow of mercury due to a vertical heated flat plate is discussed. Two numerical solutions of the relevant boundary layer equations are given in which full account has been taken of variations in density, specific heat, conductivity and viscosity with temperature. From these solutions Sparrow and Gregg have shown that flow and heat-transfer characteristics can be obtained using constant property results in conjunction with certain reference temperature relationships.

The authors feel that to understand the non-linear effects introduced by variable properties in liquids it would be more attractive to study carefully the behaviour of one specific liquid under various basic flow and heat-transfer configurations. The liquid to be used in this series of papers is water. For water, except at very high pressures or at conditions near the critical point, the properties may be taken as equal to the saturated values at the appropriate temperatures. The data for saturated water has been taken from tables recently compiled by Mayhew and Rogers [13]. A discussion of the treatment of this data is given in Appendix A. It can be seen from Table 1 that even for small temperature differences the variation in molecular viscosity is quite significant. In an extreme case the ratio of the viscosity at 0°C to that at 100°C is 6·35, and for such a temperature range it is to be expected that shear stresses and heat-transfer coefficients will be strongly dependent on the nature of the non-isothermal region of flow. Moreover it is assumed that fluid pressures and temperatures will be such that steam blanketing does not occur on solid boundaries.

With the aid of a digital computer a series of calculations on laminar forced and free convection in ducts and boundary layer flows on

Table 1

	ρ		C_p		$\mu \times 10^2$		$k \times 10^3$		$10\int_0^T k\,dT$
	Experimental Value	Formulae (A.1)	Experimental Value	Formulae (A.1)	Experimental Value	Formulae (A.1)	Experimental Value	Formulae (A.1)	Formulae (A.1)
0·01	0·99980	0·99980	1·0055	1·0055	1·782	1·782	1·316	1·316	0·00000
5	0·99990	0·99992	1·0041	1·0047	1·517	1·517	1·345	1·346	0·06660
10	0·99970	0·99970	1·0015	1·0015	1·306	1·306	1·373	1·373	0·1346
15	0·99900	0·99910	0·9996	0·9997	1·138	1·138	1·402	1·403	0·2040
20	0·99820	0·99820	0·9989	0·9988	1·002	1·002	1·431	1·431	0·2748
25	0·99701	0·99704	0·9984	0·9983	0·8903	0·8903	1·455	1·455	0·3470
30	0·99562	0·99562	0·9979	0·9979	0·7975	0·7975	1·476	1·476	0·4203
35	0·99404	0·99397	0·9977	0·9977	0·7193	0·7194	1·495	1·496	0·4946
40	0·99216	0·99216	0·9979	0·9979	0·6531	0·6531	1·514	1·514	0·5698
45	0·99020	0·99022	0·9984	0·9982	0·5963	0·5962	1·531	1·532	0·6460
50	0·98813	0·98813	0·9986	0·9986	0·5471	0·5471	1·548	1·548	0·7230
55	0·98522	0·98584	0·9989	0·9989	0·5044	0·5043	1·562	1·562	0·8007
60	0·98328	0·98328	0·9993	0·9993	0·4668	0·4668	1·574	1·574	0·8791
65	0·98039	0·98047	1·0001	0·9999	0·4338	0·4337	1·586	1·585	0·9581
70	0·97752	0·97752	1·0008	1·0008	0·4044	0·4044	1·596	1·596	1·0376
75	0·97466	0·97461	1·0015	1·0017	0·3783	0·3782	1·603	1·604	1·1176
80	0·97182	0·97182	1·0024	1·0024	0·3547	0·3547	1·610	1·610	1·1980
85	0·96899	0·96888	1·0036	1·0032	0·3336	0·3335	1·617	1·615	1·2786
90	0·96525	0·96525	1·0048	1·0048	0·3144	0·3144	1·624	1·624	1·3595
95	0·96154	0·96075	1·0060	1·0077	0·2970	0·2971	1·629	1·639	1·4411
100	0·95784	0·95784	1·0075	1·0075	0·2812	0·2812	1·631	1·631	1·5231

plane and curved surfaces will be carried out. Another interesting flow field is one which involves boundary layer separation on heated or cooled surfaces. The results using water will be different from those using air (as reported in [1]), since the variation with temperature of the viscosity of water is opposite to that of air.

The purpose of this paper is to investigate the laminar fully developed flow of water between heated vertical plates. The main reason for treating this flow configuration is that the effects of variable fluid properties on the flow and heat transfer will be easy to analyse and will not be masked as in references 8–11 by effects due to hydrodynamic and thermal entrance lengths.

2. NON-ISOTHERMAL FLOW BETWEEN PARALLEL FLAT PLATES

Consider the steady fully developed laminar flow between parallel flat plates of infinite extension in the vertical x-direction as shown schematically in Fig. 1. The plate at $y = 0$ is

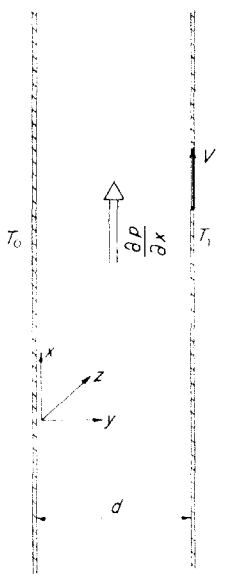

FIG. 1. Flow configuration.

fixed and maintained at temperature T_0; the plate at $y = d$ is maintained at temperature T_1 and moves with velocity V; a uniform pressure gradient $[\partial p/\partial x]$ acts in the x-direction. In all planes perpendicular to the y-direction the flow will be the same and it is assumed that the quantities describing the flow are functions of the y-ordinate only.

The governing equations of motion are:

$$\frac{\partial}{\partial x}(\rho u) = 0, \tag{1}$$

$$\frac{\partial}{\partial y}\left[\mu \frac{\partial u}{\partial y}\right] = \frac{\partial p}{\partial x} + \rho g, \tag{2}$$

$$\frac{\partial}{\partial y}\left[k \frac{\partial T}{\partial y}\right] = -\frac{1}{J}\mu\left[\frac{\partial u}{\partial y}\right]^2 - \beta \frac{Tu}{J}\frac{\partial p}{\partial x}, \tag{3}$$

where

$$\beta = -\frac{1}{\rho}\left(\frac{\partial \rho}{\partial T}\right)_p$$

is the coefficient of volumetric expansion.

The boundary conditions are:

$$\left.\begin{aligned} u = 0,\ T = T_0 \text{ at } y = 0, \\ u = V,\ T = T_1 \text{ at } y = d. \end{aligned}\right\} \tag{4}$$

The temperature dependent relations:

$$\rho = \rho(T),\ \mu = \mu(T) \text{ and } k = k(T) \tag{5}$$

are required to complete the above system of equations (see Appendix A).

Consider now equations (1)–(5). The continuity equation (1) states the assumption that the velocity and thermal profiles are fully developed. The pressure gradient $\partial p/\partial x$ is constant and all other partial derivatives in the momentum and energy equations (2) and (3) now become ordinary differentials. Apart from the non-linearity introduced by the variable fluid properties (5) these equations are coupled by virtue of the gravitational body force, viscous dissipation and the compression work term. Due to the presence of the gravitational body force it is necessary to specify the temperature of the fluid at the inlet; this is denoted by T_r.

In the usual fashion the body force is expressed in terms of the buoyancy force, on defining

$$p_D = p - p_r, \tag{6}$$

where p_r is the hydrostatic pressure that would be obtained at a particular level if the temperature of the water was constant and equal to T_r

throughout the system (see Ostrach [14]). Now $(\partial p_r/\partial x) = -\rho_r g$ and so the momentum equation (2) becomes:

$$\frac{\mathrm{d}}{\mathrm{d}y}\left[\mu\frac{\mathrm{d}u}{\mathrm{d}y}\right] = \frac{\partial p_D}{\partial x} + (\rho - \rho_r)g. \tag{7}$$

Introducing the representative velocity

$$N_r = \frac{d^2}{2}\frac{1}{\mu_r}\left[-\frac{\partial p_D}{\partial x}\right], \tag{8}$$

and the new variables:

$$Y = \frac{y}{d},\ U = \frac{u}{N_r},\ \Theta = \frac{(T - T_0)}{(T_1 - T_0)}, \tag{9}$$

these equations reduce to:

$$\frac{\mathrm{d}}{\mathrm{d}Y}\left[\frac{\mu}{\mu_r}\frac{\mathrm{d}U}{\mathrm{d}Y}\right] = -2 - \frac{Gr_r}{Re_r}\left[\frac{\rho - \rho_r}{\rho_1 - \rho_0}\right], \tag{10}$$

$$\left.\begin{aligned}\frac{\mathrm{d}}{\mathrm{d}Y}\left[\frac{k}{k_r}\frac{\mathrm{d}\Theta}{\mathrm{d}Y}\right] &= -\gamma_r\frac{\mu}{\mu_r}\left[\frac{\mathrm{d}U}{\mathrm{d}Y}\right]^2 - \\ &\frac{d^2}{k_r(T_1 - T_0)}\left[\frac{\beta T u}{J}\frac{\partial p}{\partial x}\right],\end{aligned}\right\} \tag{11}$$

subject to the boundary conditions:

$$\left.\begin{aligned}U = 0,\quad \Theta = 0,\ \text{at}\ Y = 0,\\ U = \frac{V}{N_r},\ \Theta = 1,\ \text{at}\ Y = 1.\end{aligned}\right\} \tag{12}$$

In equations (10) and (11) the Reynolds number

$$Re_r = \frac{\rho_r N_r d}{\mu_r};$$

The Grashof number

$$Gr_r = -\frac{\rho_r(\rho_1 - \rho_0)g\,d^3}{\mu_r^2};$$

and

$$\gamma_r = \frac{1}{J}\frac{\mu_r N_r^2}{k_r(T_1 - T_0)} = E_r \times Pr_r,$$

where the Eckert number

$$E = \frac{N_r^2}{JC_{pr}}(T_1 - T_0)$$

and the Prandtl number

$$Pr_r = \left[\frac{C_p\mu}{k}\right]_r.$$

To establish the order of magnitude of these terms, a constant fluid property model will be used to discuss the special case of the flow between fixed plates. Furthermore to avoid undue complications the inlet temperature is taken to be $T_r = \frac{1}{2}(T_1 + T_0)$, the arithmetic mean of the plate temperatures. The model fluid is assumed to have the properties:

$$k = k_r,\ \mu = \mu_r,\ \rho = \rho_r[1 - \beta_r(T - T_r)].^* \tag{13}$$

The variable property equations (10) to (12) become:

$$\left.\begin{aligned}\frac{\mathrm{d}^2U}{\mathrm{d}Y^2} &= -2 + \frac{Gr_r}{Re_r}\left(\tfrac{1}{2} - \Theta\right),\\ \frac{\mathrm{d}^2\Theta}{\mathrm{d}Y^2} &= -\gamma_r\left[\frac{\mathrm{d}U}{\mathrm{d}Y}\right]^2 + \\ &\frac{\beta_r N_r T_r d^2}{J(T_1 - T_0)k_r}\left[\frac{2\mu_r N_r}{d^2} + \rho_r g\right]U,\end{aligned}\right\} \tag{14}$$

subject to the conditions:

$$\left.\begin{aligned}U(0) = U(1) = 0,\\ \Theta(0) = 0,\ \Theta(1) = 1.\end{aligned}\right\} \tag{15}$$

Consider the following example when the representative velocity $N_r = 100$ cm/s, $d = \frac{1}{2}$ cm, $T_0 = 10°C$ and $T_1 = 20°C$. From Table 1, $\rho_{15} = 0{\cdot}999$ g/cm^3, $\mu_{15} = 1{\cdot}138 \times 10^{-2}$ g/cm s, $k_{15} = 1{\cdot}402 \times 10^{-3}$ cal/s cm degC and $\beta_{15} = 1{\cdot}5 \times 10^{-4}$/degC. From the above definitions $Re_r = 4{\cdot}4 \times 10^3$,† $Gr_r = 14$, $(Gr_r/Re_r) = 3{\cdot}2 \times 10^{-3}$, $\gamma_r = 1{\cdot}9 \times 10^{-4}$ and the maximum value of the compression term will be an order of magnitude less than γ_r. In this latter connection it has been shown by Hanratty *et al.* [16], who studied a similar constant fluid property model, that computed temperature profiles were unaffected by density changes except at values of Gr_r/Re_r greater than 120.

---

* In the evaluation of the order of magnitude of the compression work term in equation (11) it is sufficient to replace T by T_r.

† If the Reynolds number Re is based on the average velocity, then $Re \doteq \frac{1}{6}Re_r = 733$. In an experimental investigation on fully developed turbulent heat transfer to water in thin rectangular channels, Levy *et al.* [15] state that their test data for $Re < 10^4$ may be in the transitional region between laminar and turbulent flow.

The results to be presented in this paper on the variable fluid property flow and heat transfer in water will relate to flow regimes with buoyancy force neglected, i.e. the relevant dimensionless group $Gr_r/Re_r \ll 1$. In sacrificing this term the flow and heat transfer depend only on the four quantities d, $(\partial p_D/\partial x)$, T_0 and T_1.*

Returning now to the variable property equations (10)–(12) and on neglecting the buoyancy force term and the work done against compression these equations become:

$$\frac{\mathrm{d}}{\mathrm{d}Y}\left[\frac{\mu}{\mu_r}\frac{\mathrm{d}U}{\mathrm{d}Y}\right] = -2, \tag{16}$$

and

$$\frac{\mathrm{d}}{\mathrm{d}Y}\left[\frac{k}{k_r}\frac{\mathrm{d}\Theta}{\mathrm{d}Y}\right] = -\gamma_r\frac{\mu}{\mu_r}\left[\frac{\mathrm{d}U}{\mathrm{d}Y}\right]^2. \tag{17}$$

The suffix r is used to denote an arbitrary reference temperature taken to be $T_r = \frac{1}{2}(T_0 + T_1)$.

The thermal boundary conditions are:

$$\Theta(0) = 0,\ \Theta(1) = 1. \tag{18}$$

In the general case when the pressure gradient $\partial p_D/\partial x$ is non-zero and the upper plate moves with velocity $V = nN_r$ the boundary conditions on the velocity are:

$$U(0) = 0,\ U(1) = n, \tag{19}$$

where n is positive or negative; for example, when n is negative the upper plate velocity is adverse to the velocity induced by the pressure gradient; when $n = 0$, i.e. the upper plate is at rest, the flow is the variable property Poiseuille flow. The special case of Couette flow is obtained when $\partial p_D/\partial x = 0$ but non-zero V, and is included in the above set of equations; when the right-hand side of (16) is identically zero, $N_r = V$, i.e. $n = 1$.

A description of the numerical solution of the fourth order boundary value problem defined by equations (16)–(19) is given in Appendix B. During the course of the numerical work it was established that the effect of viscous dissipation is negligible for the laminar flow of water at $Re \leqslant 2000$.

* Otherwise for fixed T_0 and T_1 a family of solutions exist for various datum temperature levels. However, if viscous dissipation is negligible the forced and free convection flows are simply superimposed. Some calculations have been completed for the free convection contribution to the flow for various T_r, and these may be presented at a later date.

3. DEFINITIONS OF FLOW AND HEAT-TRANSFER CHARACTERISTICS

Various quantities which are of interest are now defined. The reference temperature

$$T_r = \tfrac{1}{2}(T_0 + T_1)$$

will be used throughout.

Reynolds number

$$Re_r = \rho_r \bar{u} d/\mu_r, \tag{20}$$

where the average velocity

$$\bar{u} = \frac{1}{d}\int_0^d u\,\mathrm{d}y = N_r\int_0^1 U\,\mathrm{d}Y. \tag{21}$$

Friction factor

In hydraulic calculations the pressure drop per unit of length is expressed by

$$-\left[\frac{\partial p_D}{\partial x}\right] = \zeta\,\frac{\rho_r\bar{u}^2}{2d}.$$

The quantity ζ is known as the friction factor and it is easily shown that

$$\zeta\, Re_r = 4/\int_0^1 U\,\mathrm{d}Y. \tag{22}$$

Shear stress and skin friction

The wall shear stresses are given by

$$\tau_0 = \left[\mu\frac{\mathrm{d}u}{\mathrm{d}y}\right]_{y=0} = \frac{\mu_0 N_r}{d}\left[\frac{\mathrm{d}U}{\mathrm{d}Y}\right]_{Y=0}$$

and

$$\tau_1 = \left[\mu\frac{\mathrm{d}u}{\mathrm{d}y}\right]_{y=d} = \frac{\mu_1 N_r}{d}\left[\frac{\mathrm{d}U}{\mathrm{d}Y}\right]_{Y=1}.$$

These can be made dimensionless through the definition of local skin friction coefficients. Thus

$$C_{f0} = \frac{\tau_0}{\frac{1}{2}\rho_r\bar{u}^2} \quad \text{and} \quad C_{f1} = \frac{\tau_1}{\frac{1}{2}\rho_r\bar{u}^2}$$

producing the following relations:

$$C_{f0}\,Re_r = \frac{2\mu_0}{\mu_r}\left[\frac{dU}{dY}\right]_{Y=0} \Big/ \int_0^1 U\,dy,$$
$$C_{f1}\,Re_r = \frac{2\mu_1}{\mu_r}\left[\frac{dU}{dY}\right]_{Y=1} \Big/ \int_0^1 U\,dy. \quad (23)$$

Nusselt number

A dimensionless representation of the heat-transfer results is achieved by the use of a local heat-transfer coefficient and local Nusselt number, which are written in the usual way as

$$h = \frac{q}{(T_1 - T_0)},\quad Nu = \frac{hd}{k},$$

where the heat flux

$$q = -k(dT/dy).$$

Thus at the walls:

$$Nu_0 = \left[\frac{d\Theta}{dY}\right]_{Y=0} \quad \text{and} \quad Nu_1 = \left[\frac{d\Theta}{dY}\right]_{Y=1}, \quad (24)$$

respectively.

Reynolds analogy factor

At the walls $y = 0$ and d the Reynolds analogy factors are defined by:

$$Nu_0/C_{f0}\,Re_r \quad \text{and} \quad Nu_1/C_{f1}\,Re_r,$$

respectively.

Flow rate

The flow rate per unit length of section is

$$W = \int_0^d \rho u\,dy = N_r d \int_0^1 \rho U\,dY. \quad (25)$$

4. RESULTS FROM CONSTANT FLUID PROPERTY MODEL

Equations (16)–(19) can be easily integrated for the special case of constant fluid property by setting $\mu = \mu_r$ and $k = k_r$. The results are:

$$U = Y - Y^2 + nY, \quad (26)$$

and

$$\Theta = Y\{1 - (\gamma_r/6)[3(1+n)^2(Y-1) - 4(1+n)(Y^2-1) + 2(Y^3-1)]\} \quad (27)$$

Neglecting the viscous dissipation contribution in (27) these constant fluid property results yield:

$$\left.\begin{aligned} \bar{u} &= \tfrac{1}{6} N_r(1+3n),\\ \zeta\,Re_r &= 24/(1+3n),\\ C_{f0}\,Re_r &= 12(1+n)/(1+3n),\\ C_{f1}\,Re_r &= 12(-1+n)/(1+3n),\\ Nu_0 &= Nu_1 = 1,\\ \left[\frac{Nu}{C_f\,Re_r}\right]_0 &= (1+3n)/12(1+n),\\ \left[\frac{Nu}{C_f\,Re_r}\right]_1 &= (1+3n)/12(-1+n),\\ W/(N_r d) &= \rho_r[\tfrac{1}{6} + \tfrac{1}{2} n]. \end{aligned}\right\} \quad (28)$$

The special case of Poiseuille flow is obtained when $n = 0$. For Couette flow the constant fluid property results, neglecting viscous dissipation are:

$$U = \Theta = Y \quad (29)$$

and the relevant flow and heat-transfer parameters are:

$$\left.\begin{aligned} \bar{u} &= \frac{V}{2},\\ C_f\,Re_r &= 4 \text{ for } 0 \leqslant y \leqslant d,\\ \frac{Nu}{C_f\,Re_r} &= \tfrac{1}{4} \text{ for } 0 \leqslant y \leqslant d,\\ \frac{W}{Vd} &= \tfrac{1}{2}\rho_r. \end{aligned}\right\} \quad (30)$$

5. DISCUSSION OF VARIABLE FLUID PROPERTY RESULTS FOR WATER

Flow and heat-transfer characteristics have been evaluated for a wide variety of cases. The computations have been carried out using the Bristol University IBM 1620 Computer. It must be emphasized that since viscous dissipation has been found negligible the thermal profiles for various T_0 and T_1 are evaluated without requiring knowledge of the velocity profiles. Physically this implies that heat is transferred between the plates by conduction alone. In the following discussion the abbreviations C.P.F. and V.P.F. will be adopted for denoting constant property fluid and variable property fluid results respectively. In Figs. 2–8 the constant fluid property results, based on the reference temperature

Table 2

	Temperature, T				Couette, U				Poiseuille, U		
y/d	0–10	0–40	0–100	C.P.F.	0–10	0–40	0–100	C.P.F.	0–10	0–40	0–100
0	0·0000	0·000	0·000	0·00	0·0000	0·0000	0·0000	0·0000	0·0000	0·0000	0·0000
0·05	0·5105	2·153	5·709	0·05	0·0428	0·0284	0·0156	0·0475	0·0430	0·0323	0·0203
0·10	1·020	4·285	11·29	0·10	0·0863	0·0588	0·0346	0·0900	0·0823	0·0637	0·0425
0·15	1·527	6·399	16·74	0·15	0·1305	0·0913	0·0565	0·1275	0·1179	0·0941	0·0661
0·20	2·034	8·495	22·08	0·20	0·1755	0·1259	0·0817	0·1600	0·1495	0·1229	0·0905
0·25	2·540	10·57	27·32	0·25	0·2212	0·1652	0·1102	0·1875	0·1771	0·1496	0·1151
0·30	3·044	12·63	32·48	0·30	0·2677	0·2019	0·1422	0·2100	0·2005	0·1740	0·1393
0·35	3·547	14·68	37·57	0·35	0·3149	0·2432	0·1778	0·2275	0·2195	0·1956	0·1623
0·40	4·049	16·70	42·60	0·40	0·3629	0·2869	0·2171	0·2400	0·2340	0·2139	0·1836
0·45	4·551	18·71	47·57	0·45	0·4117	0·3328	0·2601	0·2475	0·2439	0·2284	0·2023
0·50	5·051	20·70	52·49	0·50	0·4613	0·3812	0·3069	0·2500	0·2489	0·2387	0·2176
0·55	5·550	22·68	57·37	0·55	0·5116	0·4319	0·3576	0·2475	0·2490	0·2444	0·2288
0·60	6·049	24·65	62·21	0·60	0·5627	0·4850	0·4122	0·2400	0·2440	0·2448	0·2350
0·65	6·546	26·60	67·01	0·65	0·6145	0·5406	0·4709	0·2275	0·2336	0·2396	0·2354
0·70	7·042	28·55	71·79	0·70	0·6672	0·5986	0·5337	0·2100	0·2179	0·2281	0·2292
0·75	7·538	30·48	76·54	0·75	0·7207	0·6591	0·6006	0·1875	0·1965	0·2100	0·2153
0·80	8·032	32·40	81·27	0·80	0·7749	0·7222	0·6717	0·1600	0·1694	0·1846	0·1930
0·85	8·526	34·32	86·00	0·85	0·8300	0·7877	0·7472	0·1275	0·1363	0·1514	0·1613
0·90	9·018	36·22	90·70	0·90	0·8859	0·8559	0·8271	0·0900	0·0972	0·1100	0·1192
0·95	9·510	38·11	95·36	0·95	0·9425	0·9266	0·9113	0·0475	0·0518	0·0597	0·0657
1·00	10·00	40·00	100·00	1·00	1·0000	1·0000	1·0000	0·0000	0·0000	0·0000	0·0000

$T_r = \frac{1}{2}(T_0 + T_1)$, are indicated using a dashed line.

Temperature profiles

In Table 2 some representative profiles are given for $T_0 = 0°C$ and $T_1 = 10$, 40 and 100°C, respectively. It is to be expected that the difference between C.P.F. and V.P.F. thermal profiles is not appreciable since the conductivity varies slowly with the temperature. As k increases with increasing T in the interval 0–100°C, the V.P.F. temperature will always be greater than the C.P.F. temperature at any point between the plates.* For example, in an extreme case with $T_0 = 0°C$ and $T_1 = 100°C$, a maximum difference of +6·5 per cent occurs between the C.P.F. and V.P.F. temperatures at $y/d = 0{\cdot}4$. In Fig. 2 the thermal profile and related data on ρ, μ and k are given graphically for the case $T_0 = 0°C$ and $T_1 = 100°C$.

It is interesting to note that the effect of variable k on the temperature profile in water may, in fact, be much greater than that due to the viscous dissipation in flows which are laminar, i.e. $Re < 2000$. Returning to the C.P.F. example discussed in Section 2, it can be shown, on using expression (27) that when $y/d = \frac{1}{2}$ the C.P.F. model with viscous dissipation gives $T = 15{\cdot}00005°C$, whilst the V.P.F. computed value is $T = 15{\cdot}052°C$.

Velocity profiles

The effect of variable viscosity on the velocity profiles is most clearly seen from some of the computed results on Couette flow; these are given graphically in Fig. 3 and in tabular form in Table 2. If the plate at rest is maintained at temperature T_0 and the moving plate is maintained at temperature $T_1 > T_0$ then as T_1 increases the velocity at any point decreases. The reason for this is that μ decreases with increasing

* This result follows directly from equations (17) and (18). On neglecting viscous dissipation, the relevant solution is [see expression (B.11)]

$$\int_0^{\Theta} k \, d\Theta = Y \int_0^1 k \, d\Theta.$$

For the range $T_0 \leqslant T \leqslant T_1$, let

$$k = k_0(1 + \lambda\Theta), \lambda > 0.$$

Then

$$\Theta + \tfrac{1}{2}\lambda\Theta^2 = (1 + \tfrac{1}{2}\lambda)Y,$$

and there result the inequalities:

$$\left[\frac{\partial\Theta}{\partial Y}\right]_0 > 1 > \left[\frac{\partial\Theta}{\partial Y}\right]_1 \quad \text{and} \quad \Theta \geqslant Y,$$

provided $\lambda > 0$.

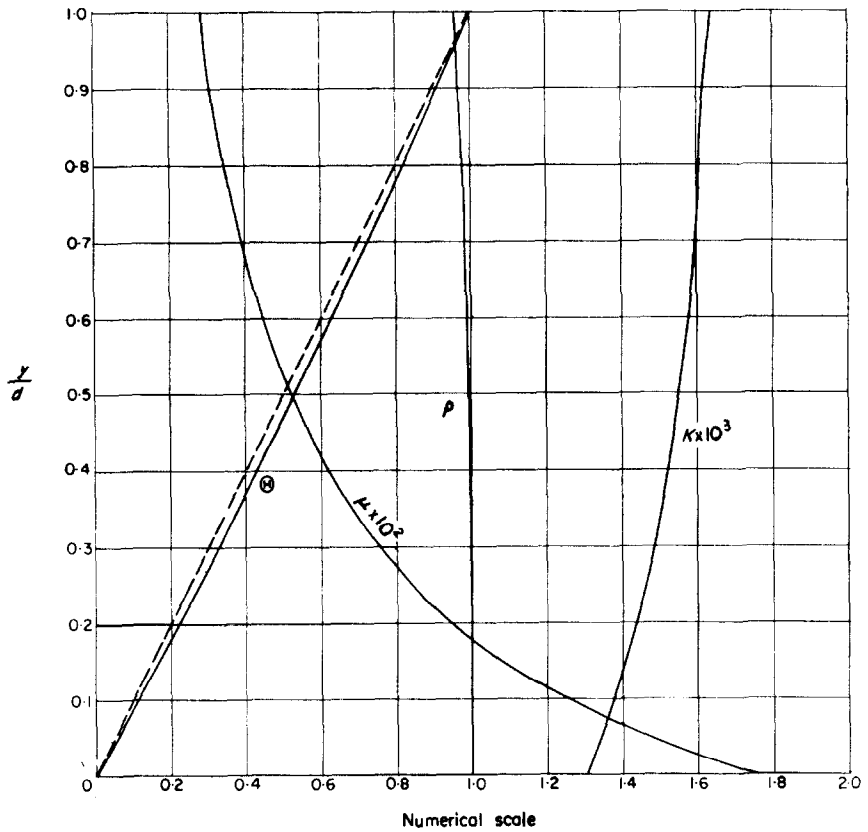

FIG. 2. Thermal profile Θ and related values of ρ, μ and k for the case $T_0 = 0°C$ and $T_1 = 100°C$.

T and so the moving hot plate exerts less shear force on the layer on fluid adhering to the plate. On the other hand if $T_1 < T_0$ and T_0 increases the velocity at any point is increased since greater shear force is transmitted to the fluid by the cold moving plate.

In Table 2 and Fig. 4 some profiles are given for the V.P.F. Poiseuille flow. The form of presentation of these results can be a little misleading due to the presence of the viscosity μ_r in the representative velocity

$$N_r = \frac{d^2}{2}\frac{1}{\mu_r}\left[-\frac{\partial p_D}{\partial x}\right].$$

A comparison of the V.P.F. profiles with the C.P.F. profile indicates that maximum velocity occurs between the central axis and the heated wall. The V.P.F. profiles can be compared with one another provided the pressure gradient and distance between the plates is the same in each case. Thus, for example, at $y/d = \frac{1}{2}$ the ratio

$$u(0, 100)/u(0, 10) = [\mu_5\, U(0.\,100)]/[\mu_{50}\, U(0, 10)] = 2{\cdot}54.$$

In fact if $\partial p_D/\partial x$ and d are kept fixed the velocity is increased on increasing the temperature of the liquid.

In Fig. 5 velocity profiles are given for mixed V.P.F. Poiseuille and Couette flows. Here the V.P.F. and C.P.F. profiles can be compared with one another since the value of the reference viscosity μ_r is the same in each case. When the plate velocity and the pressure gradient induced velocity N_r are equal (i.e. $n = 1$), it is seen that

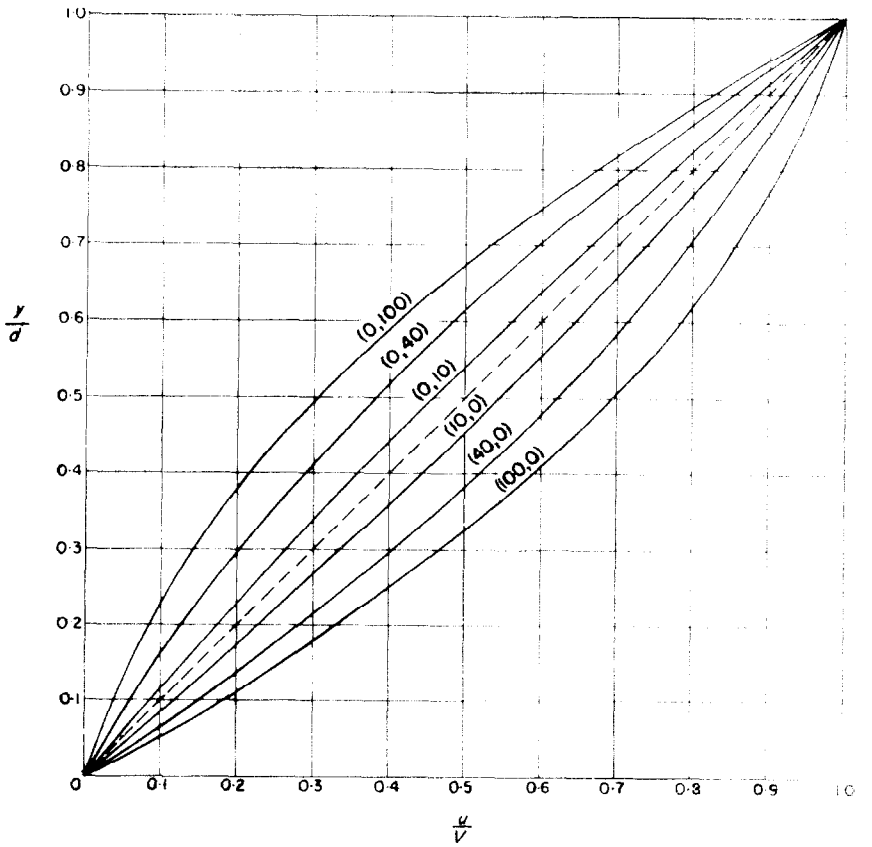

FIG. 3. Variable property velocity profiles in Couette flow for various wall temperature conditions (T_0, T_1).

velocity overshoot occurs in the V.P.F. profile for $T_0 = 100°C$ and $T_1 = 0°C$, but does not occur in the C.P.F. profile. Compared with the C.P.F. profile, the V.P.F. profile has increases in velocity due to (*a*) the supply of heat at $y = 0$ which lowers the viscosity in this region and so produces a greater pressure gradient force and (*b*) the extraction of heat by the cold moving plate at $y = d$, which now transmits greater shear force. The total contribution produces the observed velocity overshoot. When the plate velocity is adverse to that induced by the pressure gradient, then velocity undershoot is seen to occur in the profile for $T_0 = 0°C$, $T_1 = 100°C$ and $n = -1$. Velocity overshoot does not occur in the profile for $T_0 = 0°C$, $T_1 = 100°C$ with $n = 1$ as the effect of extracting heat at the fixed plate and supplying heat at the moving plate both result in a considerable reduction in velocity as compared with the C.P.F. profile; there is also a point of inflexion at $y/d = 0{\cdot}675$, which does not occur in the V.P.F. profile.

In Fig. 6 velocity profiles are given for the two cases $T_0 = 0°C$, $T_1 = 100°C$, $n = +2$ and $T_0 = 100°C$, $T_1 = 0°C$, $n = +2$, respectively. As the plate velocity is $2N_r$ the Couette flow will always dominate the Poiseuille flow. This is especially true when heat is extracted at the moving plate. It should be noted that since viscous dissipation is negligible, and the gravitational buoyancy force has been neglected in the evaluation of the velocity profiles the various solutions presented are not all independent.

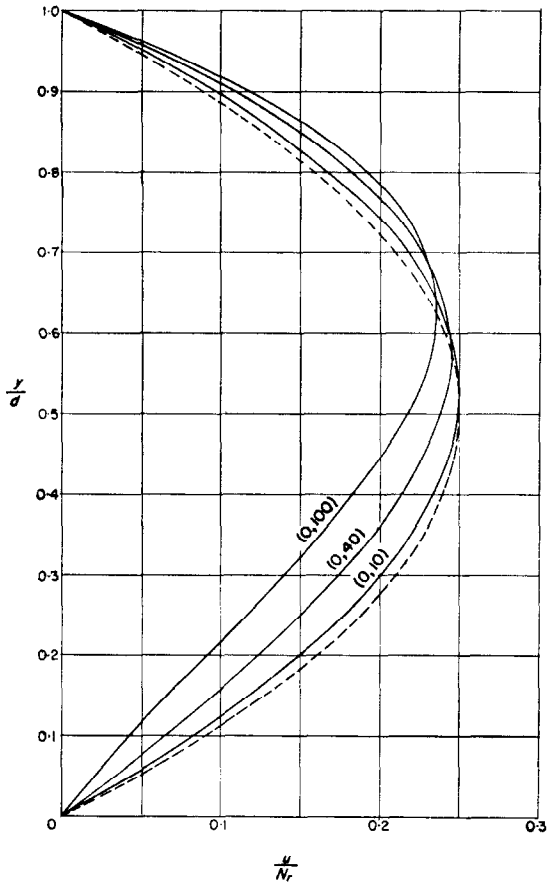

FIG. 4. Variable property velocity profiles in Poiseuille flow for various wall temperature conditions (T_0, T_1).

For mixed Poiseuille and Couette V.P.F. flow:

$$U(T_0, T_1, n; y/d) = U(T_1, T_0, / n; 1 - y/d) + n, \quad (31)$$

and for Couette V.P.F. flow:

$$U(T_0, T_1; y/d) = 1 - U(T_1, T_0; 1 - y/d). \quad (32)$$

Flow rate

For the case of Couette flow the flow rate W is given in Table 3 for various wall temperatures lying in the range 0–100°C. The quantity $W/(Vd)$ decreases when heat is supplied to the system. In particular for $T_0 = T_1 = 0$°C, $W/(Vd) = 0{\cdot}4999$ but when $T_0 = 0$°C and $T_1 = 100$°C, $W/(Vd) = 0{\cdot}3619$, a reduction of twenty-three per cent in flow rate; this is due to reduced viscosity at the heated plate as previously discussed. It should be noted that although the dimensionless average velocities $\bar{U} = \bar{u}/V$ are related by the expression

$$\bar{U}(T_0, T_1) = 1 - \bar{U}(T_1, T_0), \quad (33)$$

no such simple expression is true for $\rho\bar{U}$. For the range 0–100°C the maximum flow rate for C.P.F. Couette flow will occur when $T_0 = 100$°C and $T_1 = 0$°C. If the C.P.F. model [equation (30)] is used in this case the error in $W/(Vd)$ will be twenty-five per cent.

Numerical results for V.P.F. Poiseuille flow

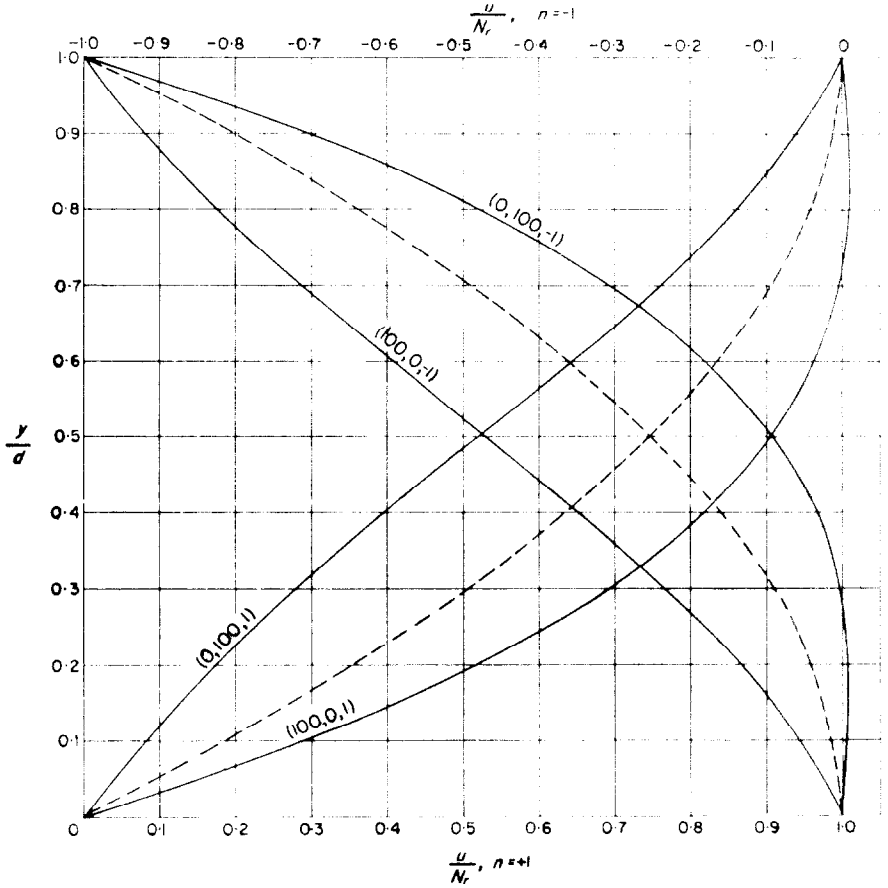

FIG. 5. Representative velocity profiles in mixed Poiseuille–Couette flow for various values of (T_0, T_1, n); $n = +1$.

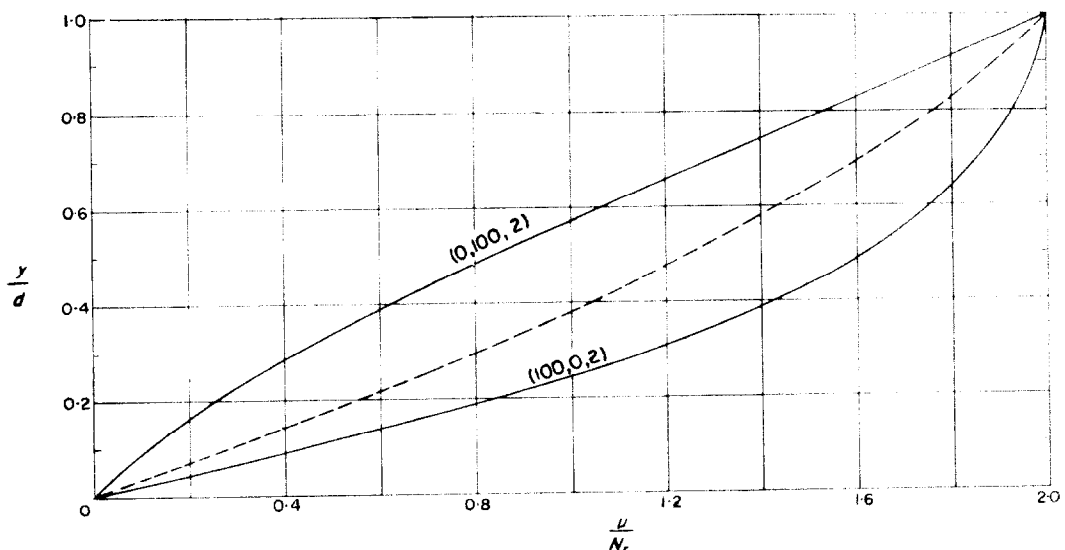

FIG. 6. Representative velocity profiles in mixed Poiseuille–Couette flow for various values of (T_0, T_1, n); $n = +2$.

Table 3

T_0	T_1	$\bar{U}$	$W/(Vd)$	$C_f Re_r$	$Nu_0/C_{f0}Re_r$	$Nu_1/C_{f1}Re_r$
0	0	0·5000	0·4999	4·000	0·2500	0·2500
	10	0·4742	0·4741	4·205	0·2432	0·2330
	40	0·4208	0·4190	4·626	0·2340	0·2033
	70	0·3903	0·3852	4·872	0·2312	0·1906
	100	0·3714	0·3619	5·037	0·2298	0·1854
10	0	0·5258	0·5257	3·792	0·2584	0·2697
	10	0·5000	$0{\cdot}4998_5$	4·000	0·2500	0·2500
	20	0·4780	0·4774	4·175	0·2446	0·2348
	40	0·4439	0·4417	4·448	0·2375	0·2154
	70	0·4097	0·4041	4·728	0·2318	0·1995
	100	0·3877	0·3774	4·919	0·2284	0·1923
40	0	0·5792	0·5783	3·362	0·2798	0·3220
	10	0·5561	0·5549	3·550	0·2699	0·2975
	30	0·5166	0·5138	3·867	0·2553	0·2620
	40	0·5000	0·4961	4·000	0·2500	0·2500
	70	0·4606	0·4527	4·319	0·2384	0·2262
	100	0·4327	0·4196	4·555	0·2303	0·2138
70	0	0·6097	0·6067	3·120	0·2977	0·3611
	10	0·5903	0·5867	3·282	0·2874	0·3339
	30	0·5550	0·5495	3·565	0·2713	0·2933
	70	0·5000	0·4888	4·000	0·2500	0·2500
	80	0·4891	0·4762	4·088	0·2458	0·2437
	100	0·4700	0·4533	4·245	0·2389	0·2337
100	0	0·6286	0·6225	2·976	0·3137	0·3889
	10	0·6123	0·6054	3·115	0·3036	0·3606
	40	0·5673	0·5569	3·475	0·2803	0·3019
	70	0·5300	0·5148	3·764	0·2635	0·2694
	100	0·5000	0·4789	4·000	0·2500	0·2500

rates are given in Table 4; in Fig. 7 the quantity $W/(N_r d)$ for $T_0 = 0$, 10, 40, 70, 100°C is plotted as a function of $T_r = \frac{1}{2}(T_0 + T_1)$. The various values computed for the range 0–100°C are bounded by the curves for $T_0 = 0$°C and 100°C and by the C.P.F. curve, which is also an envelope of the V.P.F. results. For V.P.F. Poiseuille flow $\overline{\rho U}(T_0, T_1) = \overline{\rho U}(T_1, T_0)$ and so curves for fixed T_0 intersect. Consider the results when $T_0 = 40$°C. There is a maximum in $W/(N_r d)$ at $T = 40$°C, but this does not occur in the actual flow rate W. If d and $\partial p_D/\partial x$ are kept fixed W increases monotonically with increasing T_r, i.e. with increasing thermal capacity* of the system; when

$$T_0 = 40°\text{C} \quad \text{then} \quad W \Big/ \left\{ \frac{d}{2} \left[-\frac{\partial p_D}{\partial x} \right] \right\} =$$

1·59, 1·84, 2·32, 2·55, 3·28 and 3·99

for $T_r = 20$, 25, 35, 40, 55 and 70°C, respectively. Again, if T_r, $[\partial p_D/\partial x]$ and d are kept fixed the V.P.F. flow rates are not independent of

* The thermal capacity of the system is defined as $\int_0^y \rho C_p T \, dy = \rho_r C_p T_r d$ on the C.P.F. model. The V.P.F. value will be close to this since ρ, C_p and k-data vary slowly with T.

Table 4

T_0	T_1	$\bar{U}$	$W/(N_r d)$	ζRe_r	$C_{f0}Re_r$	$C_{f1}Re_r$	Nu_0	Nu_1	$10^2 \cdot Nu_0/C_{f0}Re_r$	$10^2 \cdot Nu_1/C_{f1}Re_r$
0	0	0·1667	0·1666	24·00	12·00	−12·00	1·000	−1·000	8·333	8·333
	10	0·1660	0·1660	24·09	12·67	−11·42	1·023	−0·9798	8·072	8·577
	40	0·1597	0·1593	25·05	14·51	−10·54	$1·082_5$	−0·9407	7·470	8·924
	70	0·1526	0·1512	26·22	15·99	$-10·23_5$	1·126	−0·9288	7·047	9·075
	100	0·1465	0·1440	27·30	17·16	−10·14	$1·157_5$	−0·9337	6·745	9·208
10	0	0·1660	0·1660	24·09	11·42	−12·67	0·9798	−1·023	8·577	8·072
	10	0·1667	0·1666	24·00	12·00	−12·00	1·000	−1·000	8·333	8·333
	20	0·1661	0·1660	24·08	12·53	−11·51	1·022	−0·9804	8·152	8·518
	40	0·1631	0·1625	24·53	13·64	−10·89	1·056	−0·9581	7·744	8·800
	70	0·1569	0·1554	25·49	15·05	−10·55	1·096	−0·9431	7·283	8·942
	100	0·1510	0·1482	26·49	16·22	−10·27	1·123	−0·9458	6·928	9·210
40	0	0·1597	0·1593	25·05	10·54	−14·51	0·9408	$-1·082_5$	8·924	7·462
	10	0·1631	0·1625	24·54	10·89	−13·64	0·9581	−1·056	8·800	7·744
	30	0·1664	0·1653	24·05	11·62	−12·42	0·9875	−1·013	8·496	8·156
	40	0·1667	0·1654	24·00	12·00	−12·00	1·000	−1·000	8·333	8·333
	70	0·1647	0·1623	24·28	13·10	−11·19	1·030	−0·9771	7·862	8·735
	100	0·1608	0·1570	24·87	14·11	−10·76	1·049	−0·9740	7·438	9·052
70	0	0·1526	0·1512	26·22	10·24	$-15·98_5$	0·9288	−1·126	9·075	7·047
	10	0·1570	0·1554	25·49	10·44	−15·05	0·9431	−1·096	9·029	7·283
	30	0·1629	0·1608	24·55	$10·92_5$	−13·63	0·9671	−1·046	8·852	7·673
	70	0·1667	0·1629	24·00	12·00	−12·00	1·000	−1·000	8·333	8·333
	80	0·1665	0·1623	24·09	12·27	−11·75	1·005	−0·9962	8·188	8·479
	100	0·1654	0·1602	24·18	12·81	−11·36	1·014	−0·9921	7·914	8·731
100	0	0·1465	0·1440	27·30	10·14	−17·16	0·9337	$-1·157_5$	9·208	6·745
	10	0·1510	0·1482	26·49	10·27	−16·22	0·9458	−1·123	9·210	6·928
	40	0·1608	0·1570	24·87	10·76	−14·11	0·9740	−1·049	9·052	7·438
	70	0·1654	0·1602	24·18	11·36	−12·81	0·9921	−1·014	8·731	7·914
	100	0·1667	0·1596	24·00	12·00	−12·00	1·000	−1·000	8·333	8·333

T_0 and T_1. From Fig. 7, taking $T_r = 30°C$ $W/(N_r d) = 0·154$, 0·160, 0·166, 0·164 when $T_0 = 0$, 10, 30, 40°C, respectively. Since $\overline{\rho U}(T_0, T_1) = \overline{\rho U}(T_1, T_0)$, there will be a maximum flow rate when $T_0 = T_1 = T_r = 30°C$, i.e. when the fluid is at a uniform temperature of 30°C across the channel.

In Table 5 flow rates are given in tabular form for V.P.F. mixed Poiseuille and Couette flow when $n = \pm 1$; in Fig. 8 results are given graphically for $n = \pm 1$ and ± 2 together with the related C.P.F. values. Here the situation is complicated since a reduction in heat input increases the Couette velocity but at the same time decreases the velocity due to the pressure gradient induced Poiseuille flow. For $n = \pm 1$ and ± 2 and fixed T_0, $\partial p_D/\partial x$ and d, the flow rate increases with increasing T_r. In particular, for the C.P.F. model, the flow rate is zero when

$$n = -\tfrac{1}{3} \quad \text{or} \quad V = -\tfrac{1}{3}\frac{d^2}{2\mu_r}\left[-\frac{\partial p_D}{\partial x}\right].$$

Typical results for the V.P.F. (computed using Tables 2 and 3) are: $T_0 = 0°C$ and $T_1 = 10$, 40, 70, 100°C, $n = -0·3502$, $-0·3801$, $-0·3926$ and $-0·3979$, respectively; $T_0 = 100°C$ and $T_1 = 0$, 10, 40, 70°C, $n = -0·2314$, $-0·2448$,

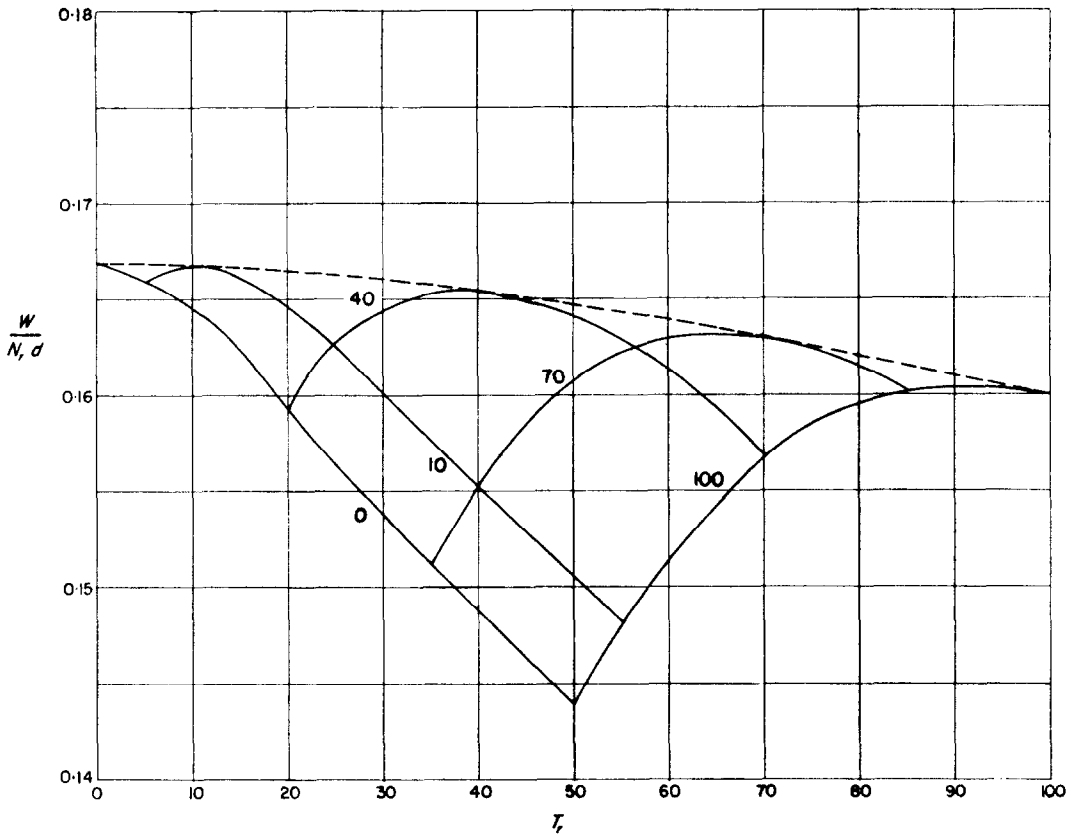

FIG. 7. Variable property Poiseuille flow rates for various values of T_0 as a function of $T_r = \frac{1}{2}(T_0 + T_1)$.

$-0{\cdot}2819$ and $-0{\cdot}3111$, respectively. These results indicate that when heat is supplied at the moving plate, a larger adverse velocity is required for the V.P.F. than in the C.P.F. model to produce zero flow rate.

Nusselt number

The heat flux across the channel is constant and is independent of the flow rate. In Table 4 the wall Nusselt numbers Nu_0 and Nu_1 are given, and these are simply related by the expression:

$$\frac{Nu_0}{Nu_1} = \frac{k_1}{k_0}; \tag{34}$$

it follows from (34) that $Nu_0 > Nu_1$ if $T_0 < T_1$, since k increases with increasing T. When $T_0 = 0°C$ and $d = 1$ cm, the heat flux q_1 [defined by expressions (24)] required to produce the temperatures $T_1 = 10$, 40, 70, 100°C are 485, 2052, 3731, 5460 kcal/m^2 h, respectively.

Friction factor, skin friction coefficient and Reynolds analogy factor

These various dimensionless quantities are given in Tables 3, 4 and 5 for Poiseuille, Couette and mixed Poiseuille–Couette flow respectively.

For Poiseuille flow the dimensionless group $\zeta\, Re_r$ varies slowly for fixed T_0 and variable T_1. Hence if $\partial p_D/\partial x$ and d are kept constant the friction factor ζ will decrease when heat is supplied to the flow. The skin friction coefficients C_{f0} and C_{f1} follow the same trend although the rate of decrease at the cold wall will be much less than that at the heated wall. It should be noted that the absolute magnitudes of the wall

Table 5

T_0	T_1	$n = +1$ $\bar{U}$	$W/(N_r d)$	ζRe_r	$C_{f0}Re_r$	$C_{f1}Re_r$	$n = -1$ $\bar{U}$	$W/(N_r d)$	ζRe_r	$C_{f0}Re_r$	$C_{f1}Re_r$
0	0	0·6667	0·6665	6·000	6·000	0·0000	−0·3333	−0·3333	−12·00	0·0000	12·00
	10	0·6402	0·6401	6·248	6·400	0·1518	−0·3081	−0·3081	−12·98	0·3550	12·63
	40	0·5805	0·5783	6·890	7·345	0·4541	−0·2611	−0·2598	−15·32	1·416	13·90
	70	0·5429	0·5365	7·368	7·995	0·6272	−0·2378	−0·2340	−16·82	2·257	14·56
	100	0·5179	0·5058	7·723	8·467	0·7437	−0·2249	−0·2179	−17·78	2·861	14·92
10	0	0·6919	0·6919	5·782	5·623	−0·1581	−0·3598	−0·3597	−11·12	0·2702	11·39
	10	0·6667	0·6665	6·000	6·000	0·0000	−0·3333	−0·3333	−12·00	0·0000	12·00
	20	0·6441	0·6441	6·210	6·340	0·1301	−0·3119	−0·3114	−12·82$_5$	0·2954	12·53
	40	0·6069	0·6069	6·590	6·918	0·3278	−0·2808	−0·2792	−14·24$_5$	0·8906	13·35
	70	0·5666	0·5664	7·059	7·585	0·5261	−0·2528	−0·2487	−15·82	1·677	14·14
	100	0·5388	0·5388	7·424	8·086	0·6616	−0·2367	−0·2292	−16·90	2·288	14·61
40	0	0·7389	0·7376	5·414	4·913	−0·5005	−0·4194	−0·4191	−9·535	0·6284	10·16
	10	0·7192	0·7174	5·562	5·214	−0·3477	−0·3930$_5$	−0·3924	−10·18	0·5062	10·68
	30	0·6829	0·6791	5·857	5·757	−0·1003	−0·3503	−0·3484	−11·42	0·1838	11·60
	40	0·6667	0·6614	6·000	6·000	0·0000	−0·3333	−0·3307	−12·00	0·0000	12·00
	70	0·6253	0·6149	6·397	6·632	0·2353	−0·2959	−0·2904	−13·52	0·5676	12·95
	100	0·5935	0·5766	6·739	7·144	0·4048	−0·2719	−0·2627	−14·71	1·096	13·62
70	0	0·7622	0·7580	5·248	4·544	−0·7041	−0·4571	−0·4555	−8·751	0·7450	9·496
	10	0·7472	0·7421	5·353	4·786	−0·5676	−0·4333	−0·4314	−9·230	0·6879	9·918
	30	0·7179	0·7104	5·571	5·235	−0·3363	−0·3921	−0·3887	−10·20	0·5070	10·71
	70	0·6667	0·6517	6·000	6·000	0·0000	−0·3333	−0·3292	−12·00	0·0000	12·00
	80	0·6556	0·6385	6·101	6·167	0·0655	−0·3226	−0·3139	−12·40	0·1375	12·26
	100	0·6354	0·6134	6·295	6·476	0·1811	−0·3045	−0·2931	−13·13$_5$	0·4109	12·72
100	0	0·7751	0·7665	5·161	4·331	−0·8301	−0·4821	−0·4785	−8·298	0·7990	9·097
	10	0·7633	0·7536	5·240$_5$	4·531	−0·7097	−0·4612	−0·4572	−8·672	0·7728	9·445
	40	0·7281	0·7139	5·493	5·084	−0·4094	−0·4064	−0·3999	−9·841	0·5912	10·43
	70	0·6954	0·6750	5·751$_5$	5·572	−0·1799	−0·3646	−0·3546	−10·97	0·3156	11·29
	100	0·6667	0·6386	6·000	6·000	0·0000	−0·3333	−0·3193	−12·00	0·0000	12·00

Reynolds analogy factors are not identical for a V.P.F.; in the case of $T_0 = 0°C$ and $T_1 = 100°C$ these differ by 37 per cent.

In Couette flow the shear stress at any point across the channel is constant and so the skin friction coefficients will be the same at both fixed and moving plates. Once again, for fixed V and d, the skin friction coefficient is reduced when heat is supplied to the system. Reynolds analogy is exact in this case since both shear stress and heat flux remain constant at any point across the channel. The difference between the wall Reynolds analogy factors quoted in Table 3 is due to the definitions taken for Nu_0 and Nu_1; in fact

$$k_0\, Nu_0/C_{f0}\, Re_r = k_1\, Nu_1/C_{f1}\, Re_r. \quad (35)$$

For mixed Poiseuille–Couette flow shear friction coefficients are given for $n = +1$ and $n = -1$. These are useful as a guide for deciding the appropriate wall temperatures producing velocity overshoot when $n = +1$, and velocity undershoot when $n = -1$. Obviously these effects will occur when the skin friction coefficients have opposite signs; for example, when $T_0 = 40°C$:

velocity overshoot occurs when $n = +1$, $T_1 < 40°C$, i.e. by cooling the moving plate;

velocity undershoot occurs when $n = -1$, $T_1 > 40°C$, i.e. by heating the moving plate.

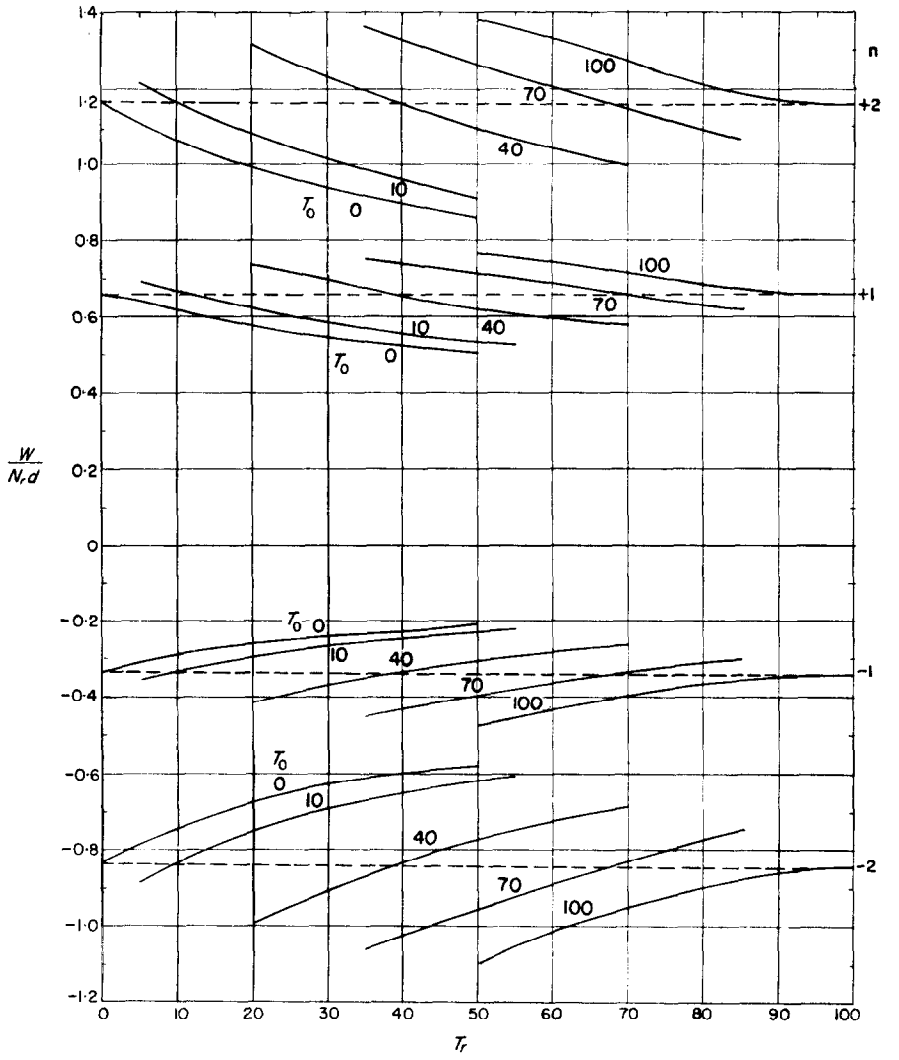

FIG. 8. Variable property flow rates in mixed Poiseuille–Couette flow for various values of T_0 as a function of $T_r = \frac{1}{2}(T_0 + T_1)$.

REFERENCES

1. K. STEWARTSON, The *The Theory of Laminar Boundary Layers in Compressible Fluids*. Oxford Mathematical Monographs, Clarendon Press, Oxford (1964).
2. G. VOGELPOHL, Der Übergang der Reibungswärme von Lagern aus der Schmierschicht in die Gleitflächen—Temperaturverteilung und thermische Anlaufstrecke in parallelen Schmierschichten bei Erwärmung durch innere Reibung, *Forschungsh. Ver. Dtsch Ing.* 425 (1949).
3. R. NAHME, Beiträge zur hydrodynamischen Theorie der Lagerreibung, *Ing.-Arch.* **11**, 191 (1940).
4. H. HAUSENBLAS, Die nicht isotherme Stromung einer zähen Flüssigkeit durch enge Spalte und Kapillarröhren. *Ing.-Arch.* **18**, 151 (1950).
5. S. M. TARG, Basic problems in the theory of laminar flow. Gostikhizdat, Moscow (1951).
6. R. G. DEISSLER, Analytical investigation of fully developed laminar flow in tubes with heat transfer with fluid properties variable along the radius, *NACA TN* 2410 (1951).
7. S. M. MASLEN, On fully developed laminar flows: some solutions and limitations, and effects of compressibility, variable properties, and body forces, *NASA TR R*-34 (1959).

8. L. M. K. BOELTER, V. H. CHERRY, H. A. JOHNSON and R. C. MARTINELLI, *Heat Transfer Notes*, Chapter X. University of California Press (1948).
9. K. YAMAGATA, A contribution to the theory of non-isothermal laminar flow of fluids inside a straight tube of circular cross section, *Mem. Fac. Engng, Kyushu* **8** (6), 365 (1940).
10. R. L. PIGFORD, Non-isothermal flow and heat transfer inside vertical tubes, *Chem. Engng Progr. Symposium Series* **51** (17), 79 (1955).
11. K. T. YANG, Laminar forced convection in liquids in tubes with variable viscosity, *J. Heat Transfer*, **84**, 353 (1962).
12. E. M. SPARROW and J. L. GREGG, The variable property problem in free convection, in *Recent Advances in Heat and Mass Transfer*, Ed. J. P. HARTNETT, p. 353. McGraw-Hill, New York (1961).
13. Y. R. MAYHEW and G. F. C. ROGERS, *Thermodynamic and Transport Properties of Fluids, MKS Units*. Blackwell, Oxford (1964).
14. S. OSTRACH, Laminar natural convection flow and heat transfer of fluids with and without heat sources in channels with constant wall temperature, *NACA TN* 2863 (1952).
15. S. LEVY, R. A. FULLER and R. O. NIEME, Heat transfer to water in thin rectangular channels, *J. Heat Transfer*, **81**, 129 (1959).
16. T. J. HANRATTY, E. M. ROSEN and R. L. KABEL, *Industr. Engng Chem.* **50**, 815 (1958).

APPENDIX A

Data for saturated water

The data for saturated water have been taken from tables recently compiled by Mayhew and Rogers [13]; the smoothed experimental values of the density, specific heat, viscosity and conductivity for $0 \leqslant T \leqslant 100°C$ are given in Table 1 in metric units. Although the specific heat data is not used in the present paper, it has been included for completeness and will be used in later work.

There are two methods of fitting data of the above type: (*a*) by collocation and (*b*) by the method of least squares. The theoretical expression used can take the form of either an algebraic expression or a series of orthogonal polynomials. Each of these methods have well-known pitfalls, especially when the data has an appreciable scatter. If this is the case, method (*b*) must be employed. However, the data for saturated water are now accurately known and possibly only the last figure quoted may be in error. Thus the method of collocation is used.

Algebraic expressions are chosen in the form:

$$\left.\begin{aligned} \rho &= \sum_{i=0}^{n} A_i\theta^i,\ C_p = \sum_{i=0}^{n} B_i\theta^i, \\ \mu &= \sum_{i=0}^{n} \exp(C_i\theta^i),\ k = \sum_{i=0}^{n} \exp(D_i\theta^i) \end{aligned}\right\} \quad (A.1)$$

where $\theta = (T - 50)/50$.

Consider the ρ-data in the range 0–100°C. If $n = 2$ values of ρ at $T = 0$, 50 and 100°C are used to determine A_0, A_1 and A_2; n is increased by 2 and ρ values at $T = 0(25)100$°C are used to determine the A_i for $i = 0(1)4$. The calculation is then repeated with $n = 10$ and 20. It is found that these theoretical expressions improve in accuracy with increasing n provided $n \leqslant 10$. The accuracy being checked on comparing values obtained using the theoretical expression with experimental values at points intermediate to those used in the fitting process. However, when $n = 10$, unavoidable small oscillations begin to appear in the theoretical expression at these points. For $n = 20$ these oscillations have quite alarming amplitudes, especially near the end points at $T = 0$ and 100°C. For this reason the value of the derivative $d\rho/dT$, evaluated using the theoretical expression, is in serious error when n is large.

The results for $n = 10$ have been accepted for the ρ-data and as can be seen in Table 1 are in error by less than 0·1 per cent. Similar accuracy for the C_p-data was achieved with $n = 10$. The μ-data have been fitted precisely, as this data has already been smoothed in [13] after taking logarithms. For the k-data with $n = 10$ the accuracy obtained was $<0{\cdot}1$ per cent for $0 \leqslant T < 85$°C. The theoretical expressions reveal a spurious maximum near 95°C. In fact a rather diffuse maximum does occur in the experimental data in the range 115–135°C. It is possible that these spurious oscillations found in the theoretical expressions near 100°C could be avoided by fitting in the range 0–140°C and using the expressions for the range 0–100°C only.

It is interesting to note that the inversion temperature near 4°C has been adequately predicted by the ρ-expression. For problems involving forced convection an accuracy of

Table 6

i	A_i	B_i	C_i	D_i
0	0·988 130	0·988 610	−5·208 294	−6·470 986
1	−0·021 761	0·003 382	−0·836 625	0·095 773
2	−0·010 265	−0·002 976	0·228 220	−0·069 060
3	−0·013 377	0·004 571	−0·072 689	0·027 692
4	−0·001 000	0·081 685	0·036 071	0·204 396
5	0·064 100	−0·026 187	−0·025 843	−0·145 549
6	0·037 889	−0·275 517	−0·041 654	−0·793 563
7	−0·096 266	0·034 689	0·018 216	0·309 234
8	−0·078 639	0·384 833	0·072 355	1·126 945
9	0·046 325	−0·015 495	−0·006 439	−0·179 732
10	0·042 705	−0·180 145	−0·037 178	−0·523 533

$<0{\cdot}1$ per cent in the fitting procedure is sufficient for all practical purposes; the coefficients A_i, B_i, C_i, D_i and $i = 0(1)10$ for saturated water are given in Table 6. However, for free convection flows a more careful appraisal of the ρ-data is required, especially in the range 0°C–10°C.

APPENDIX B

Numerical solution of equations (16)–(19)

New variables y_1 and y_2 are introduced as follows:

$$y_1 = \Theta \quad \text{and} \quad y_2 = \frac{k}{k_r} y_1', \tag{B.1}$$

where the prime denotes differentiation with respect to Y. The boundary value problem defined by equations (8)–(10) is then equivalent to the system of first order equations:

$$y_1' = \frac{k_r}{k} y_2, \; y_1(0) = 0, \tag{B.2}$$

$$y_2' = -\gamma_r \frac{\mu_r}{\mu} (\beta - 2(Y - \tfrac{1}{2}))^2, \; y_2(0) = \alpha, \tag{B.3}$$

$$y_3' = -2(Y - \tfrac{1}{2}) \frac{\mu_r}{\mu}, \; y_3(0) = 0, \tag{B.4}$$

$$y_4' = \frac{\mu_r}{\mu}, \; y_4(0) = 0. \tag{B.5}$$

where

$$\gamma_r = \frac{1}{J} \frac{N_r^2 \mu_r}{k_r (T_1 - T_0)}$$

is a dimensionless constant. The dimensionless velocity is

$$U = y_3(Y) + \beta\, y_4(Y). \tag{B.6}$$

In the above system of equations the unknown constants of integration α and β are determined such that the conditions $\Theta(1) = 1$ and $U(1) = n$ are satisfied. It follows that

$$y_1(1) = 1, \tag{B.7}$$

and

$$\beta = [n - y_3(1)]/y_4(1), \tag{B.8}$$

and so the equations (B.2)–(B.5), together with the conditions (B.7) and (B.8) must be solved by an iterative scheme.

Except in the case of high viscosity oils, the parameter γ_r is small and so for most liquids a first approximation to the above equations is obtained by putting $\gamma_r = 0$. On neglecting viscous dissipation ($\gamma_r = 0$) in equation (B.3)

$$y_2(Y) = \alpha = \text{const.} \tag{B.9}$$

and (B.2) becomes

$$y_1' = \frac{k}{k_r} \alpha, \; y_1(0) = 0. \tag{B.10}$$

On elementary integration and using condition (B.7),

$$\alpha = \frac{1}{k} \int_0^1 k \, dy_1,$$

or in terms of the physical variables:

$$\alpha = \frac{1}{k_r(T_1 - T_0)} \int_{T_0}^{T_1} k(T)\,dT. \qquad (B.11)$$

Given the theoretical expression for the k-data the constant α is determined by numerical integration; in Table 1 the $\int_0^T k\,dT$ is tabulated for water. Equations (B.10), (B.4) and (B.5) are integrated simultaneously and β is calculated using expression (B.8). Using this value of β equations (B.2) and (B.3) for non-zero γ_r are solved, by an iterative method, to determine α consistent with (B.7). Once a new value of α is available the equations (B.2)–(B.5) are solved simultaneously to determine from (B.8) the next estimate of β. This process is repeated until the required accuracy is obtained in y_1, y_3 and y_4, i.e. in Θ and U.

For the special case of Couette flow equation (B.3) is replaced by:

$$y_2' = -\gamma_r \frac{\mu_r}{\mu} \beta^2,\ y_2(0) = 0, \qquad (B.12)$$

equation (B.4) is omitted and the condition (B.8) is replaced by

$$\beta = \frac{1}{y_4(1)}. \qquad (B.13)$$

The procedure already described for solving the more general equations (B.2)–(B.8) is also applicable to this case.

The numerical integration of the above first order equations may be performed using the Runge–Kutta method. Once U and Θ are known with accuracy the dimensionless average velocity $\bar{U}$ and the dimensionless mass flow $(1/\rho_r)\overline{\rho U}$ are found on integrating the first order equations:

$$y_5' = y_3,\ y_5(0) = 0, \qquad (B.14)$$

$$y_6' = y_4,\ y_6(0) = 0, \qquad (B.15)$$

$$y_7' = \frac{\rho}{\rho_r} y_3,\ y_7(0) = 0, \qquad (B.16)$$

and

$$y_8' = \frac{\rho}{\rho_r} y_4,\ y_8(0) = 0. \qquad (B.17)$$

In the general case with pressure gradient occurring:

$$\bar{U} = \int_0^1 U\,dY = y_5(1) + \beta\, y_6(1)$$

$$\frac{1}{\rho_r}\overline{\rho U} = \frac{1}{\rho_r}\int_0^1 \rho U\,dY = y_7(1) + \beta\, y_8(1); \qquad (B.18)$$

for Couette flow only equations (B.15) and (B.17) are integrated, yielding:

$$\bar{U} = y_6(1)/y_4(1),\ \frac{1}{\rho_r}\overline{\rho U} = y_8(1)/y_4(1) \qquad (B.19)$$

Résumé—L'écoulement laminaire entièrement développé d'eau dans une conduite verticale est examiné, en employant les équations complètes du mouvement avec les valeurs expérimentales (dans la gamme 0–100°C) pour la viscosité, la conductivité, la chaleur spécifique et la densité. Bien que les effets locaux des variations de ces quantités sont évidemment faibles, l'effet cumulatif est sensible pour des différences de température modérées. En conséquence, on a insisté sur l'évaluation des propriétés intégrées telles que le flux de masse et le transport de chaleur.

Des écoulements de Poiseuille, de Couette et de Poiseuille–Couette (mixtes) sont examinés pour une gamme de différences de températures pariétales et les effets de la dépendance de ces propriétés en fonction de la température sur les profils de vitesse et de température sont discutés en détail. Les nombres de Nusselt pariétaux, les débits, les coefficients de frottement, les coefficients de perte de charge et les facteurs d'analogie de Reynolds sont examinés pour tous ces régimes.

Zusammenfassung—Unter Verwendung der vollständigen Bewegungsgleichungen mit Versuchswerten (im Bereich von 0° bis 100°C) für die Zähigkeit, Leitfähigkeit, spezifische Wärmekapazität und Dichte wird die ausgebildete laminare Strömung von Wasser in einem senkrechten Kanal untersucht. Obwohl die lokale Auswirkung bei Änderungen diesser Grössen natürlich klein ist, wird ihr Gesamteinfluss bei geringen Temperaturunterschieden bedeutend. Demnach wurde der Berechnung der Integralgrössen wie Massenstrom und Wärmeübergang besondere Bedeutung beigemessen.

Poiseuille-, Couette- und gemischte Poiseuille-Couetteströmungen werden für einen Bereich von Wandtemperaturunterschieden untersucht und die Einflüsse der temperaturabhängigen Stoffgrössen auf die Geschwindigkeits- und thermischen Profile im einzelnen diskutiert. Für alle diese Bereiche werden Wandnusseltzahlen, Strömungsgeschwindigkeiten, Oberflächenreibungsbeiwerte, Reibungsbeiwerte und analoge Reynoldszahlen berechnet.

Аннотация—Рассматривается полностью развитое ламинарное течение воды в вертикальном канале с помощью системы уравнений движения, используя экспериментальные значения (в области от 0° до 100°С.) вязкости, теплопроводности, удельной теплоемкости и илотности. Не смотря на то, что локальные изменения этих величин незначительны, их общий эффект существенен для средних температурных разностей. В соответствии с этим, обращалось особое внимание на оценку интегральных характеристик, таких как поток массы и теплообмен.

Исследовались течения Пуазейля, Куэтта и смешанное течение Пуазейля–Куэтта в некотором диапазоне перепадов температуры у стенки. Подробно рассматривалось влияние зависимых от температуры свойств на профили скорости и температуры. Для всех режимов произведен рассчет чисел Нуссельта у стенки, массового расхода жидкости, коэффициентов поверхностного трения, трения и аналогии Рейнольдса.